The Perfectly Matched Layer as Lateral Boundary in Finite-Difference Transmission-Line Analysis

Thorsten Tischler, *Student Member, IEEE,* and Wolfgang Heinrich, *Senior Member, IEEE*

***Abstract*—Using a perfectly matched layer (PML) as lateral boundary in waveguide analysis introduces artificial modes and other unexpected effects. This paper presents results of a finite-difference frequency-domain approach and an analytical investigation of the PML's capability to simulate the lateral open space, including an accuracy estimation. A criterion how to detect the desired modes out of the mode spectrum is also given. The findings are verified for a coplanar waveguide radiating into the substrate.**

***Index Terms*—Coplanar waveguides, electromagnetic propagation in absorbing media, electromagnetic radiation effects, finite-difference methods.**

I. Introduction

AMONG THE absorbing boundary conditions used with the finite-difference (FD) or finite-element (FE) methods, the currently most powerful formulation is the perfectly matched layer (PML) approach. Two types of PML are to be distinguished: the split-field formulation, introduced by Berenger [1] and the anisotropic-material-based description by Sacks *et al.* [2]. Both provide absorbing properties for any frequency and angle of incidence. The anisotropic-material PML formulation offers the special advantage that it does not require modification of Maxwellian equations. Hence, it can be implemented easily in frequency-domain FD and FE codes, and it preserves consistency of Maxwellian equations. This is important because, for instance, mode orthogonality in a waveguide is maintained, which is not clear for the split-field approach.

Both types of PMLs and their properties have been studied extensively in the literature during the last years (e.g., [3]–[5]). To the authors knowledge, however, none of these contributions treats the waveguide case, where the PML acts as lateral boundary of a longitudinally homogeneous structure. This is presented in this paper. Starting from a PML implementation, according to [2] into a finite-difference frequency-domain (FDFD) approach, this paper addresses the following three basic questions.

- How does the PML boundary change the mode spectrum of the waveguide structure?
- How can one identify the waveguide modes of interest?
- How accurate does the PML describe the leakage effects and, thus, attenuation due to radiation?

Manuscript received March 1, 2000; revised August 21, 2000.

The authors are with the Ferdinand-Braun-Institut für Höchstfrequenztechnik, D-12489 Berlin, Germany (e-mail: tischler@fbh-berlin.de; w.henrich@ieee.org).

Publisher Item Identifier S 0018-9480(00)10712-4.

Our investigations revealed some unexpected results that needed support by an analytical treatment. The analytical findings are compared to numerical data for the case of a coplanar waveguide (CPW), which radiates into the substrate.

Although this paper focuses on the frequency domain, the results are relevant for the finite difference time domain (FDTD) as well because the mode phenomena influence the time-domain behavior equally, even if they do not appear there in a distinct and unambiguous way.

II. Implementation of the Anisotropic PML

The PML is implemented into our well-proven in-house FDFD software [6]. Waveguide analysis is formulated as an eigenvalue problem for the complex propagation constant. As the code has the capability to handle anisotropic lossy media, PML implementation is straightforward. We use the discrete integral form of Maxwellian equations

$$\oint_{\partial\Omega} \vec{H}\, d\vec{s} = \int_{\Omega} j\omega[\underline{\varepsilon}]\vec{E}\, d\vec{\Omega}$$
$$\oint_{\partial\Omega} \vec{E}\, d\vec{s} = -\int_{\Omega} j\omega[\underline{\mu}]\vec{H}\, d\vec{\Omega} \tag{1}$$

applied to each elementary cell, together with the well-known PML diagonal permittivity and permeability tensors, of the form

$$[\underline{\varepsilon}] = \varepsilon \begin{bmatrix} \eta & 0 & 0 \\ 0 & \eta^{-1} & 0 \\ 0 & 0 & \eta \end{bmatrix} \quad [\underline{\mu}] = \mu \begin{bmatrix} \eta & 0 & 0 \\ 0 & \eta^{-1} & 0 \\ 0 & 0 & \eta \end{bmatrix} \tag{2}$$

with $\eta = 1 - j\zeta$ and $\zeta = (\kappa/\omega\varepsilon_0)$.

These tensors are valid for a PML acting in the y-direction, as is assumed in Fig. 1.

III. What About the Mode Spectrum?

What type of mode spectrum can we expect for a waveguide structure with lateral PML layers? Since there is always an electric or magnetic wall behind the PML, the entire structure forms a closed waveguide, which is partly filled with an artificial anisotropic material. If this PML material was not be present, we would have a huge number of box modes that are related to the enclosing box rather than to the actual transmission-line structure we are interested in.

Ideally, introducing the PML should suppress these box modes, leaving only the modes guided by the transmission-line structure. However, since the total number of modes is constant (at least in the FD formulation), the PML cannot remove any mode, but only shift them into other parts of the eigenvalue spectrum. Hence, the question arises how the undesired box modes are influenced when introducing the PML. In order to

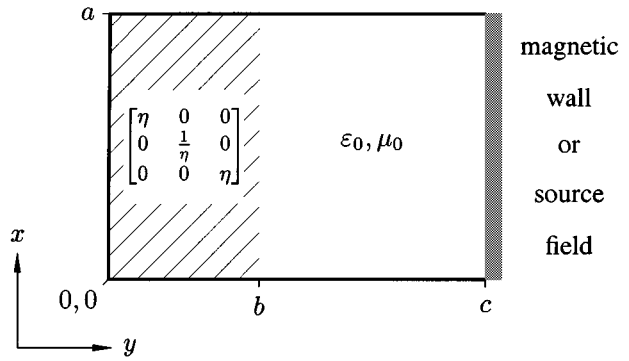

Fig. 1. Partly PML-filled rectangular waveguide (the dimensions are $a = 140$ mm, $b = 80$ mm, and $c = 200$ mm).

clarify this, in Section IV, we consider a simple structure that can be treated analytically.

IV. Analytical Model Partly PML-Filled Rectangular Waveguide

Fig. 1 shows the structure to be investigated, i.e., a rectangular waveguide, which is partly filled with the PML. The upper and lower boundaries at $x = 0$ and $x = a$ as well as the left-hand-side one at $y = 0$ are formed by electric walls, the right-hand-side boundary at $y = c$ is a magnetic wall. The left-hand-side part of the cross section with $0 < y \leq b$ is filled with the anisotropic PML material. The propagation characteristics of this structure can be derived analytically. Accounting for the special properties of the PML layer (see (2), one finds that TE_z and TM_z modes exist, which are degenerated as for the isotropic homogeneous waveguide. The solution for the propagation constant k_z reads

$$k_{zmn} = \sqrt{\omega^2 \mu_0 \varepsilon_0 - \left(\frac{m\pi}{a}\right)^2 - \frac{\left(n+\frac{1}{2}\right)^2 \left(\frac{\pi}{b}\right)^2}{\left(1 - j\frac{b}{c}\zeta\right)^2}} \qquad (3)$$

with $m = 0, 1, 2, \ldots$ and $n = 0, 1, 2, \ldots$.

It should be noted that due to the $(n+1/2)$ term in (3) a TE_{00} mode exists. In Fig. 2, the k_z eigenvalues of three TE_{mn} modes (TE_{01}, TE_{02}, and TE_{11}) are plotted in the complex plane with conductivity κ as a parameter. The real part of k_z represents the phase constant, the imaginary part the attenuation constant. Increasing conductivity κ from zero to ∞, the attenuation shows a maximum at an intermediate κ value. Thus, attenuation is limited and much smaller than the phase constant, i.e., not as high as is desirable. Moreover, the maximum decreases with frequency and differs significantly from mode to mode. This means: the PML shifts the propagation constants along the β-axis and leads to some attenuation α. However, it does not cause the box modes to become so strongly attenuated that they can easily be separated from the desired guided modes by considering α.

V. Finding the Guided Modes

In order to introduce a useful criterion to separate the waveguide modes of interest from the box modes, we use the rectangular waveguide of Fig. 1 as an example. With the magnetic

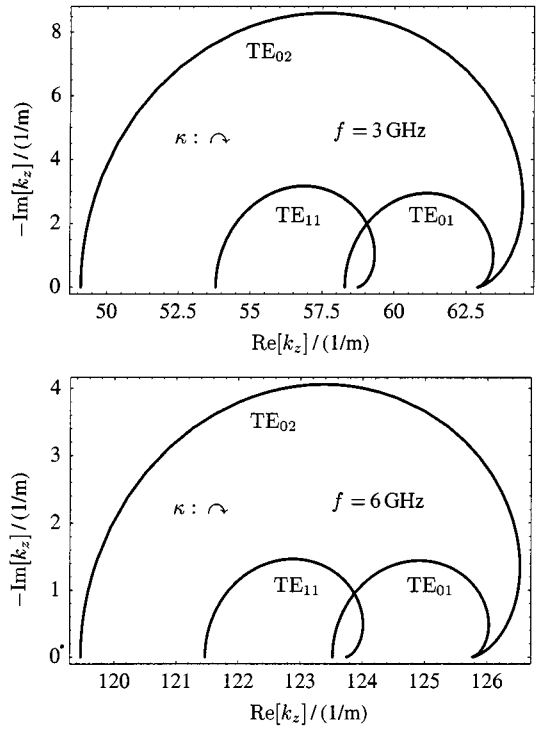

Fig. 2. Propagation constant k_z in the complex plane with conductivity κ [see (2)] as parameter, for two frequencies of 3 and 6 GHz, respectively (TE_{01}, TE_{02}, and TE_{11} mode of the structure in Fig. 1).

wall on the right-hand side, one has a waveguide supporting TE_z and TM_z modes according to (3). Introducing a source field $E_{x0}(x,z) = E_0 e^{-jk_{zs}z}$ as the right-hand-side boundary at $y = c$, on the other hand, yields an analytical approximation for the case where a guided mode with propagation constant k_{zs} radiates laterally toward the PML region. In this case, the field components can be derived using a TE_z-wave ansatz. For a complete solution, both the source-induced fields and the mode fields have to be considered.

In order to identify certain modes, we calculate the z-directed power flow in the PML section and the isotropic section separately

$$P_{\mathrm{PML}} = \int_0^b \int_0^a \left[E_x^{(1)} H_y^{(1)*} - E_y^{(1)} H_x^{(1)*}\right] dx\, dy$$
$$P_{\mathrm{isotropic}} = \int_b^c \int_0^a \left[E_x^{(2)} H_y^{(2)*} - E_y^{(2)} H_x^{(2)*}\right] dx\, dy \qquad (4)$$

where the superscript (1) denotes the field components inside the PML region, whereas the superscript (2) refers to components outside, i.e., in the isotropic free-space region.

We found that comparing the power flow in the PML section to that in the non-PML one provides a very useful criterion to sort out the undesired modes caused by the surrounding PML boundary. For this purpose, the quantity PPP (power part in PML)

$$\mathrm{PPP} = \left|\frac{P_{\mathrm{PML}}}{P_{\mathrm{PML}} + P_{\mathrm{isotropic}}}\right|, \qquad \text{with} \quad \mathrm{PPP} \in [0,1] \qquad (5)$$

is introduced.

In the following, our analytical example is used to demonstrate the effectiveness of the power-flow criterion. First, we have to classify the different modes according to their relevance

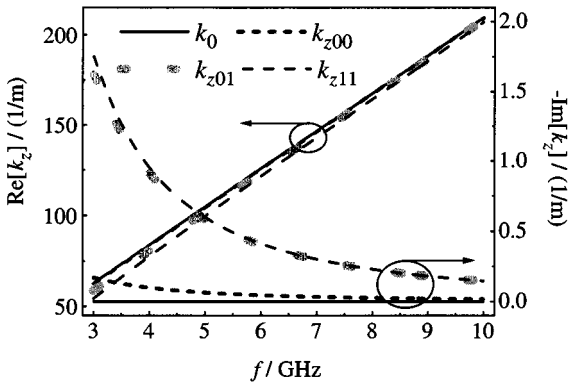

Fig. 3. Complex propagation constant $k_z = \beta - j\alpha$ of the waveguide in Fig. 1 with a magnetic wall against frequency; k_0 denotes the free-space value, k_{zmn} refers to the TE_{mn} modes [see (3)].

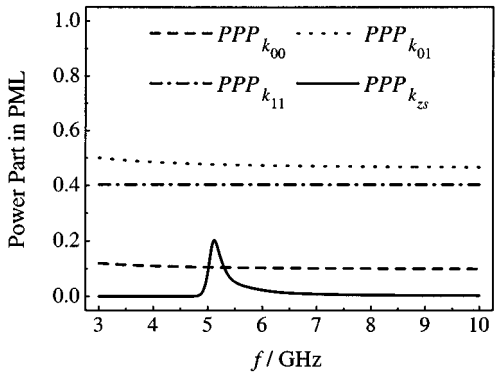

Fig. 4. PPP as a function of frequency for the TE_{00}, TE_{01}, TE_{11} mode and for the source field.

in a typical open waveguide structure: The source-field case corresponds to the waveguide mode radiating laterally into the background structure. Additionally, one has the TE_{mn} and TM_{mn} modes (the TE_{mn} notation refers to (3)). Among them, the TE_{00} mode is similar to the parallel-plate mode, i.e., a realistic mode, whereas the modes of higher order, such as TE_{01} or TE_{11} are determined by the PML and surrounding box. Those modes are parasitic and are to be separated from the desired ones.

For a first inspection, Fig. 3 presents the frequency dependence of the complex eigenvalues of the three modes TE_{00}, TE_{01}, and TE_{11}, the last two of them being artificial. A fixed conductivity value $\kappa = 0.0764$ S/m is used. Obviously, none of the modes is strongly attenuated. With growing frequency, the imaginary parts approach each other such that a separation between the eigenvalues of the desired TE_{00} mode and the parasitic TE_{01} and TE_{11} mode becomes very difficult. This problem can be overcome when considering the PPP value according to (5). As can be seen from Fig. 4, the desired modes (TE_{00} and the source field) may be easily distinguished from the undesired ones (TE_{01} and TE_{11}). The field components of the source field are calculated using a fixed value $k_{zs} = 2\pi f_0\sqrt{\varepsilon_0\mu_0}$, with $f_0 = 5$ GHz. In the whole frequency range, even at the resonant frequency $f_0 = 5$ GHz, where the guided mode is radiating very strongly into the PML region, there is a clear gap between the PPP values of the waveguide fields and the box modes. For example, PPP < 0.3 may serve as a criterion. This demonstrates usefulness of the PPP quantity.

VI. Accuracy Limitations of the PML

The structure in Fig. 1 can be used to check accuracy limits of the PML approach as well. For this purpose, we will concentrate on the case of a guided mode with the real propagation constant k_{zs}, which radiates laterally into the PML region. This is equivalent to the source field case at the right-hand-side boundary with $E_{x0}(x,z) = E_0 e^{-jk_{zs}z}$, which emulates a weakly attenuated guided wave.

This source radiates in $-y$-direction and one can calculate the resulting E_x and H_z components at the boundary between the PML and PML-free area ($y = b$). E_x and H_z can be related by an impedance Z_b, which is very helpful in discussing PML properties

$$Z_b = \left.\frac{E_x^{(1)}}{H_z^{(1)}}\right|_{y=b} = \left.\frac{E_x^{(2)}}{H_z^{(2)}}\right|_{y=b}. \tag{6}$$

For Z_b, using the field components for the source field, one obtains

$$Z_b = j\omega\mu_0 \frac{1}{\sqrt{k_0^2 - k_z^2}} \tan\left(\eta\sqrt{k_0^2 - k_{zs}^2}\, b\right) \tag{7}$$

with $\eta = 1 - j\kappa/(\omega\varepsilon_0)$ and $k_0^2 = \omega^2\mu_0\varepsilon_0$.

For $k_{zs} < k_0$, which is the case where the guided wave with propagation constant k_{zs} radiates into the PML, the impedance Z_b approaches the free-space value for increasing κ and, thus, the PML acts as the absorbing boundary. More precisely, the real part of Z_b becomes

$$\mathrm{Re}\,[Z_b] = \frac{\omega\mu_0}{\sqrt{k_0^2 - k_{zs}^2}} \cdot \frac{\sinh\left(\dfrac{2\kappa}{\omega\varepsilon_0}\sqrt{k_0^2 - k_{zs}^2}\right)}{\cos\left(2\sqrt{k_0^2 - k_{zs}^2}\right) + \cosh\left(\dfrac{2\kappa}{\omega\varepsilon_0}\sqrt{k_0^2 - k_{zs}^2}\right)} \tag{8}$$

for $k_{zs} < k_0$.

For $k_{zs} > k_0$, on the other hand, the guided mode cannot radiate into the structure and, hence, only evanescent fields are incident on the PML. In this case, as is well known, the PML fails to simulate open space. What is new, however, is that a detailed look into the real part of the impedance Z_b reveals that it may assume negative values (see the sin term in the numerator of (9)).

$$\mathrm{Re}[Z_b] = \frac{\omega\mu_0}{\sqrt{k_{zs}^2 - k_0^2}} \cdot \frac{\sin\left(\dfrac{2\kappa}{\omega\varepsilon_0}\sqrt{k_{zs}^2 - k_0^2}\, b\right)}{\cos\left(\dfrac{2\kappa}{\omega\varepsilon_0}\sqrt{k_{zs}^2 - k_0^2}\, b\right) + \cosh(2\sqrt{k_{zs}^2 - k_0^2}\, b)} \tag{9}$$

for $k_{zs} > k_0$.

In order to check the absorbing properties of the PML, we compare these $\mathrm{Re}[Z_b]$ values with the value $\mathrm{Re}[Z_{b,\mathrm{OpenSpace}}]$

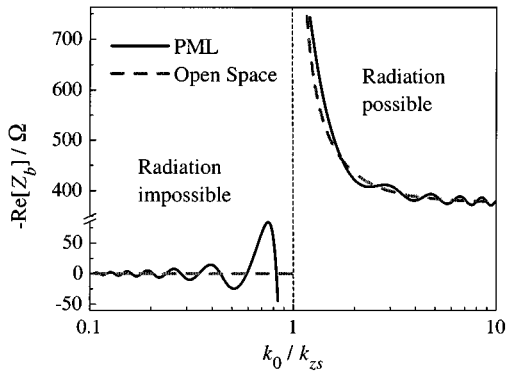

Fig. 5. Field impedance Z_b at the PML boundary [see (8) and (9)] and corresponding open space value [see (10)] for a source field with propagation constant k_{zs} (structure of Fig. 1, k_0 denotes the free-space wavenumber).

for open space. Assuming a TE_z-wave formulation, the open-space impedance $Z_{b,\mathrm{OpenSpace}}$ reads

$$Z_{b,\mathrm{OS}} = \left.\frac{E_x^{(1)}}{H_z^{(1)}}\right|_{y=b} = \begin{cases} \dfrac{\omega\mu_0}{\sqrt{k_0^2 - k_{zs}^2}}, & \text{for } k_0 > k_{zs} \\ j\dfrac{\omega\mu_0}{\sqrt{k_{zs}^2 - k_0^2}}, & \text{for } k_0 < k_{zs}. \end{cases} \tag{10}$$

In Fig. 5, these reference $Z_{b,\mathrm{OpenSpace}}$ values are plotted together with the PML ones. In the range $k_0 > k_{zs}$, where the guided mode radiates into the structure, the PML approximates open space with good accuracy, although there are still small oscillating deviations around the open-space curve. These differences are not due to numerical accuracy problems, but represent an inherent PML property caused by the finite PML thickness b. For $k_0 < k_{zs}$, where radiation is not possible, the $\mathrm{Re}[Z_b]$ values of the PML are oscillating around the zero line, which represents the open-space value. Due to the oscillating behavior, however, partly negative values for $\mathrm{Re}[Z_b]$ are found. $\mathrm{Re}[Z_b] < 0$, however, means that the PML acts as an active medium. As a consequence, evanescent fields of a guided mode reaching the PML are amplified and reflected back, which may result in negative attenuation values of the guided mode. This is exactly what we observed in FDFD analysis: for modes that cannot radiate into the background, the attenuation decreases down to very low values. In this range, attenuation may also become negative, which is again not due to numerical accuracy problems, but to finite PML thickness.

VII. Verification CPW Radiation

In order to clarify in which way the analytical observations in the previous sections affect waveguide analysis, we investigated a coplanar structure radiating into the substrate. Using our FDFD approach, we calculated effective permittivity $\varepsilon_{r,\mathrm{eff}}$ and attenuation constant α of a CPW on a silicon substrate ($\varepsilon_r = 11.67$) of infinite extent. CPW ground-to-ground spacing is 40 μm with 16-μm center-conductor width. Ground metallization is assumed to be infinite, and the conductors are ideal and infinitely thin. A graded mesh of 94 $\times$ 81 cells is used, which includes ten cells of the PML at the outer boundaries. In Fig. 6, the attenuation constants $\alpha \sim \mathrm{Im}[k_z]$ of all modes within a given range of α are plotted. It is obvious that the desired CPW

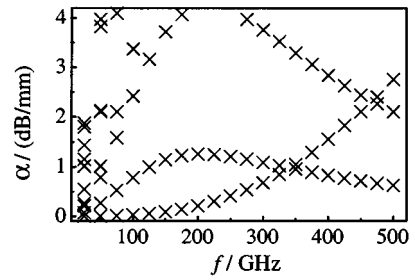

Fig. 6. Attenuation values of the eigenvalue spectrum of a CPW with infinite ground metallizations on an infinitely thick substrate.

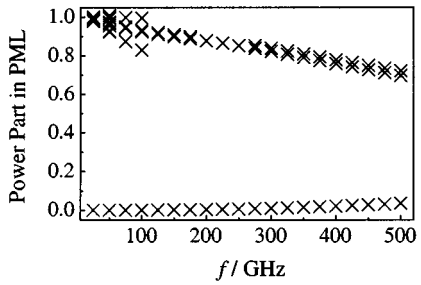

Fig. 7. PPP values for the data in Fig. 6. The lower values belong to a single mode (CPW mode), whereas the upper values belong to several modes.

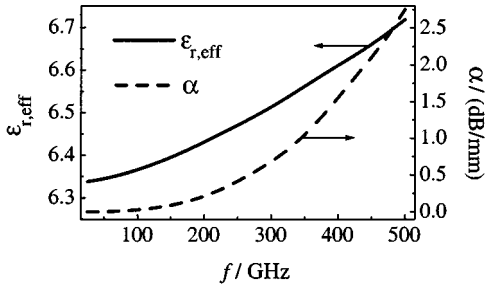

Fig. 8. Propagation constants of the CPW mode [structure with 16-μm-wide center conductor and 40-μm ground-to-ground spacing on lossless silicon substrate with $\varepsilon_r = 11.67$ (ground width and substrate infinite)].

mode cannot be easily identified when referring solely to its attenuation-constant information. Hence, an additional criterion has to be established. Fig. 7 presents the corresponding data for the PPP quantity introduced in (5). One finds that only the CPW mode exhibits a power part clearly below 0.1 over the whole frequency range, while the other PML-related modes are well separated, showing PPP values above 0.6. Thus, choosing the relation $\mathrm{PPP} > 0.3$ as a criterion for nonphysical modes, the desired CPW mode can easily be picked out of the mode spectrum. Fig. 8 shows the resulting well-known ([7], [8]) propagation characteristics. Fig. 9 adds a plot of the CPW E-field pattern at the frequency $f = 500$ GHz, which illustrates the absorbing properties of the lateral PML layers.

The power criterion proves to be a useful instrument in separating physical and nonphysical modes without further *a priori* information. It can be implemented in the eigenvalue search code and, thus, causes only small numerical overhead.

One should note that at low frequencies ($f < 0.25$ GHz) where attenuation is very small, the numerical simulation yields both negative and positive attenuation values α depending on

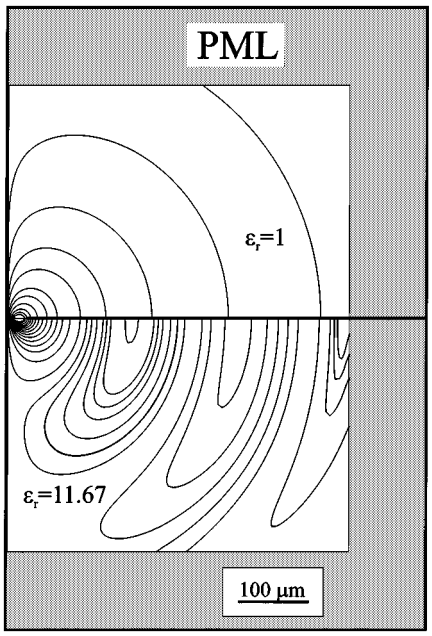

Fig. 9. E-field pattern of right-hand-side half of the CPW at $f = 500$ GHz (for the parameters see Fig. 8).

frequency. This is in accordance with the accuracy problems of the PML discussed in Section VII. Since the magnitude of α is very small, however, this effect becomes visible only for special cases.

Regarding the limitations of the PPP-based criterion, the most critical situation is that of strongly radiating modes. Usually, this occurs in the high-frequency range. The PPP values of the physical and nonphysical modes then approach each other and the decision-making algorithm may not accept only the desired modes. Thus far, the only way to handle such a situation is to include additional information, e.g., field intensity plots.

VIII. Conclusions

Applying a PML as lateral boundary in waveguide analysis involves some of the following specific effects that need to be taken into account for a proper use.

- Generally, the parasitic box modes are only weakly attenuated by the PML layer. Thus, one commonly has several modes within a given range of the propagation constant, and attenuation cannot be applied as a criterion to select the desired modes. Instead, we propose to use the part of the power flow within the PML region for this decision. This criterion proved its usefulness in practical waveguide analysis, using the FD method in frequency domain.
- There are certain differences between a PML layer and open space, which are not due to numerical peculiarities, but a PML-inherent property, related to its finite thickness. These deviations can be proven analytically.
- PML layers fail to absorb evanescent fields. In such a case, small nonphysical negative attenuation values may be observed. Naturally, this becomes apparent particularly for weakly or nonradiating modes.

Adapting the formulation according to these characteristics, the PML proves to be a useful and efficient absorbing boundary condition also for open waveguide analysis and leaky-wave structures [9].

Acknowledgment

The authors would like to thank Dr. G. Hebermehl, Weierstraβ-Institut für Angewandte Analysis und Sochastik, Berlin, Germany, and Dr. H. Zscheile, Ferdinand Braun Institut für Hochstfrequenztechnik, Berlin, Germany, for their work on the FDFD Code and helpful discussions.

References

[1] J. P. Berenger, "A perfectly matched layer for the absorption of electromagnetic waves," *J. Comput. Phys.*, vol. 114, pp. 185–200, Oct. 1994.
[2] Z. S. Sacks, D. M. Kingsland, R. Lee, and J.-F. Lee, "A perfectly matched anisotropic absorber for use as an absorbing boundary condition," *IEEE Trans. Antennas Propagat.*, vol. 43, pp. 1460–1463, Dec. 1995.
[3] M. Kuzuoglu and R. Mittra, "Frequency dependence of the constitutive parameters of causal perfectly matched anisotropic absorbers," *IEEE Microwave Guided Wave Lett.*, vol. 6, pp. 447–449, Dec. 1996.
[4] A. C. Polycarpou and C. A. Balanis, "An optimized anisotropic PML for the analysis of microwave circuits," *IEEE Microwave Guided Wave Lett.*, vol. 8, pp. 30–32, Jan. 1998.
[5] L. Zhao and A. C. Cangellaris, "GT-PML: Generalized theory of perfectly matched layers and its application to the reflectionless truncation of finite-difference time-domain grids," in *IEEE MTT-S Int. Microwave Symp. Dig.*, vol. 2, 1996, pp. 569–572.
[6] G. Hebermehl, R. Schlund, H. Zscheile, and W. Heinrich, "Eigen mode solver for microwave transmission lines," *COMPEL–Int. J. Comput. Math. Electr. Electron. Eng.*, vol. 16, no. 2, pp. 108–122, 1997.
[7] M. Y. Frankel, S. Gupta, J. A. Valdmanis, and G. A. Mourou, "Terahertz attenuation and dispersion characteristics of coplanar transmission lines," *IEEE Trans. Microwave Theory Tech.*, vol. 39, pp. 910–915, June 1991.
[8] N.-H. Huynh and W. Heinrich, "FDTD analysis of sub-millimeter wave CPW with finite-width ground metallization," *IEEE Microwave Guided Wave Lett.*, vol. 7, pp. 414–416, Dec. 1997.
[9] T. Tischler and W. Heinrich, "The perfectly matched layer as lateral boundary in finite-difference transmission-line analysis," in *IEEE MTT-S Int. Microwave Symp. Dig.*, vol. 1, 2000, pp. 121–124.

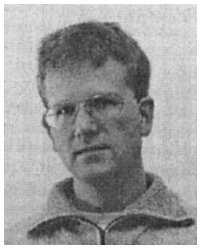

Thorsten Tischler (S'00) was born in Siegen, Germany, in 1968. He received his Diploma degree in electrical engineering from the University of Siegen, Siegen, Germany, in 1997, and is currently working toward the Ph.D. degree at the Ferdinand-Braun-Institut für Höchstfrequenztechnik, Berlin, Germany, where his doctoral work concerns the field of electromagnetic simulation.

His current focus is on the development of absorbing boundary conditions for the FDFD method.

Wolfgang Heinrich (M'84–SM'95) was born in Frankfurt/Main, Germany, in 1958. He received the Dipl.-Ing., Dr.-Ing., and habilitation degrees from the Technical University of Darmstadt, Darmstadt, Germany, in 1982, 1987, and 1992, respectively.

In 1983, he joined the staff of the Institut für Hochfrequenztechnik, Technical University of Darmstadt, where he was involved in the field-theoretical analysis and simulation of planar transmission lines. Since April 1993, he has been with the Ferdinand-Braun-Institut für Höchstfrequenztechnik, Berlin, Germany, where he is Head of the Microwave Department. His current research activities focus on electromagnetic simulation, monolithic-microwave integrated-circuit (MMIC) design for both GaAs and SiGe with emphasis on the coplanar concept, and flip-chip packaging.